crystals

MDPI

Article

Axial Compressive Behavior of Reinforced Concrete (RC) Columns Incorporating Multi-Walled Carbon Nanotubes and Marble Powder

Abdul Jalil Khan [1], Liaqat Ali Qureshi [1], Muhammad Nasir Ayaz Khan [2,*], Akhtar Gul [3], Muhammad Umar [4], Aneel Manan [4], Yasir Irfan Badrashi [3], Asim Abbas [3], Usman Javed [5,6] and Rashid Farooq [6,*]

1 Department of Civil Engineering, University of Engineering & Technology Taxila, Punjab 47080, Pakistan; abdul.jalil@students.uettaxila.edu.pk (A.J.K.); liaqat.qureshi@uettaxila.edu.pk (L.A.Q.)
2 Department of Civil Engineering, HITEC University Taxila, Punjab 47080, Pakistan
3 Department of Civil Engineering, University of Engineering & Technology Peshawar (Campus 3), Peshawar 25120, Pakistan; akhtar.wazir@uetpesh.edu.pk (A.G.); yasir_badrashi@uetpeshawar.edu.pk (Y.I.B.); asimabbas@uetpeshawar.edu.pk (A.A.)
4 Department of Civil Engineering, Swedish College of Engineering & Technology Wah Cantt, Punjab 47000, Pakistan; umarcivil11@gmail.com (M.U.); aneelmanan1@gmail.com (A.M.)
5 School of Civil and Mechanical Engineering, Curtin University, Perth, WA 6102, Australia; usman.javed1@postgrad.curtin.edu.au
6 Department of Civil Engineering, International Islamic University, Islamabad 44000, Pakistan
* Correspondence: nasir.ayaz@hitecuni.edu.pk (M.N.A.K.); rashid.farooq@iiu.edu.pk (R.F.)

check for updates

Citation: Khan, A.J.; Ali Qureshi, L.; Khan, M.N.A.; Gul, A.; Umar, M.; Manan, A.; Badrashi, Y.I.; Abbas, A.; Javed, U.; Farooq, R. Axial Compressive Behavior of Reinforced Concrete (RC) Columns Incorporating Multi-Walled Carbon Nanotubes and Marble Powder. *Crystals* **2021**, *11*, 247. https://doi.org/10.3390/cryst11030247

Academic Editors: Yixiang Gan and Nichola Coleman

Received: 15 January 2021
Accepted: 25 February 2021
Published: 28 February 2021

Abstract: In this study, Multiwalled Carbon Nanotubes (MWCNTs) and Marble Powder (MP) have been utilized in reinforced concrete columns to assess their structural behavior. The nanotubes from 0.025% to 0.20% and 5% MP by weight of cement were used. The compressive strength of reinforced concrete columns and cubes was analyzed as the main property. The incorporation of MWCNTs and marble powder was able to increase the compressive strength of columns by 72.69% and mortar by 42.45% as compared to reference concrete. The ductility was noted to be improved by 42.04%. The load-deformation and stress-strain behaviors were also analyzed. The Scanning Electron Microscopy (SEM) analysis revealed the formation of a strong compact bridge (90–100 layers), Calcium Silicate Hydrate (C-S-H) gel, evenly dispersion, and bridging effect caused by MWCNTs. The incorporation of 0.20% MWCNTs by weight of cement was recommended to be effectively used as a reinforcing agent in concrete.

Keywords: multi-walled carbon nanotubes (MWCNTs); reinforced concrete (RC) column; calcium silicate hydrate (C-S-H); marble powder; cement; concrete

1. Introduction

Concrete is being widely used as a construction material that bears various types of loading causing micro-cracking which enhances its vulnerability toward severe exposure conditions. The brittle nature of concrete induces micro-cracking that may reduce the service life of a structure due to higher penetration of intruding agents causing durability concerns. However, the carbon nanotubes were developed first in 1959 and it was used in cement-composites from the early 1990s onward [1]. Carbon nanotubes CNTs cement-composite enhanced the cement paste matrix and reduce the micro-cracks, thus increases the toughness of the cement paste matrix and high durability resistance. The properties and unique characteristics of CNTs exponentially enhance the properties of concrete. The nanoparticles act as a filler and bridges the pores at the nano level, thus improve the concrete properties [2]. In past decades, researchers have focused on developing efficient types of concrete to minimize the impact of severe loadings. Columns play important role in the ductility and strength behavior of concrete structures. Thus, it was required to

develop concrete materials which possess high energy absorption capacity to reflect more strength, ductility, and nearly inert to high loadings [3–6].

The carbon nanotubes are considered one of the best nanomaterials with extraordinary multi-properties. The CNTs are divided into two groups named Single-walled Carbon Nanotubes (SWCNTs) and Multi-walled Carbon Nanotubes (MWCNTs) [7,8]. In the recent past, several studies have investigated the effects on construction materials by the addition of CNTs. An exceptional improvement was noted in the mechanical properties of concrete by adding a small number of CNTs [9]. It was reported that adding CNTs in epoxy mortars enhances the flexural strength, toughness, young's modulus, and fracture strain [10–12]. CNTs have a tensile strength up to 11–59 GPa, which is almost 90 times greater than conventional steel. The modulus of elasticity of the carbon nanotube is about 1 terapascal (TPa) [13]. CNTs have outstanding chemical and mechanical properties, which make them ultra-high-strength material. However, a little study has been done on CNT strengthened cementitious composites because of their low production and high price. Large-scale production of CNTs now promises the use of CNTs as a structural material. Some scholars have also investigated CNT reinforced high-performance concrete. Though, different assumptions have been found concerning the strengthening of cement matrix with MWCNTs. CNTs are susceptible to create agglomerates and develop bundle structures. Appropriate mixing and distribution methods are significant factors altering the behavior of Nanocomposites, as inadequate mixing of MWCNTs leads to several imperfections in the cement matrix and reduces the strengthening effect of the MWCNTs. There exist several methods to disperse CNTs properly in a mix as the properties of concrete widely depend upon the dispersion techniques. These methods include mixing of mortar directly with CNTs in rotary mixer [14], dispersion of CNTs via ultra-sonication in presence of some polymers [15], direct mixing [16], water suspension of CNTs via ultra-sonication [17], and scattering via surfactants [18], scattering over the probe and acid-treated CNTs [19]. Published literature has reported the multi-functional performance of cement paste composite such as self-sensing [20], enhancing flexure toughness, ductility [21], microstructural crack capturing [22], and increasing the fire performance of concrete [23].

Industrial growth and revolution lead to the consumption of natural resources with the production of waste materials that target our environment. Researchers have been focused on utilizing industrial waste materials for engineering purposes. MP (MP) is industrial processing waste generated during cutting, sawing, grinding, and polishing of marble. Because of having a low concentration of reactive silica [24], it is not highly pozzolanic in nature as it acts as a nucleating agent to provide nucleation sites for precipitation of CSH gel in concrete. It also fills in the micro-sized pores present in concrete due to its microscopic nature. Therefore, MP collectively densifies the concrete microstructure by nucleation action as well as filler effect. It is thereby suggested that the MP has been successively used in concrete to improve its mechanical properties [25]. The utilization of MP in concrete and mortar up to 10% as a filler material that exhibits high strength. Further, it was observed that MP used in early ages as fill materials has a positive effect on the properties of concrete [26]. Incorporating waste powder in polymer concrete with grain size 0.075–0150 mm exhibits higher physical and mechanical properties [27]. It was examined that incorporating 60% marble wastes in concrete improves its mechanical properties [28].

It is evident from the literature [21] that the MWCNTs impart higher flexural rigidity and ductility in concrete members due to having ultra-high tensile strength. Alongside acknowledging these properties of MWCNTs cement-based composite, this research has been focused on analyzing the actual axial behavior of reinforced concrete columns containing MWCNTs along with the inclusion of MP as a filler. Therefore, the interaction of MWCNTs in cement paste matrix and their contribution toward compressive strength has been studied. The failure modes of scaled columns were analyzed alongside the determination of ductility and post-peak behavior of the reinforced concrete in compression, whereas the evidence of increased axial capacity was endorsed by the findings of Scanning Electron Microscopic (SEM) analysis of concrete microstructure containing MWCNTs.

2. Significance of Research

In the past, sufficient research has been carried out to assess the effect of mixing MWCNTs and MP separately in concrete but their combined effect on the structural behavior of columns was not studied. This study investigated the analysis of experimental results including failure mode identification, post-peak behavior of columns, strain energy absorption mechanism by comparing toughness in axial compression case, and microstructural analysis to study the microscopic behavior of MWCNTs in the strength development mechanism of reinforced concrete columns. MWCNTs are considered the best nanomaterial for improving the properties of concrete by adding a very small amount. It was expected that MWCNTs and MP would be able to improve the axial compressive behavior of RC columns as well as other parameters like crack patterns, failure modes, load-deflection curves, stress-strain behavior.

3. Experimental Program

3.1. Materials

3.1.1. Cement

In this study type, I cement under the brand name of "Fauji Cement" (Fauji Cement Company Limited, Attock, Pakistan) was used as a binder, which complies with ASTM standard specifications C150 [29]. The cement was fresh, free from impurities and lumps. The chemical properties of cement are given in Table 1 and physical properties are given in Table 2.

Table 1. Chemical composition of cement and MP.

Material	SiO_2	TiO_2	Al_2O_3	Fe_2O_3	MnO	MgO	CaO	Na_2O	K_2O	P_2O_5
Cement	21	0.348	5.04	3.24	0.064	2.56	61.7	0.252	1.117	0.068
Marble Powder	1.83	-	0.56	0.24	-	1.08	52.34	0.01	0.17	-

Table 2. Physical properties of materials used.

Material	Fineness (cm^2/g)	Water Absorption (%)	Specific Gravity	Setting Time (min)		Compressive Strength MPa	
				Initial	Final	7 Days	28 Days
Cement	2915	-	2.99	97	195	24.3	36.24
Fine Aggregates	-	1.22	2.73	-	-	-	
Coarse Aggregates	-	0.44	2.83	-	-	-	
Marble Powder	3450	0.95	2.70	-	-	-	

3.1.2. Aggregates

Fine aggregates (F.A) were collected from Lawrencepur deposits in Pakistan. The fineness modulus of FA was found as 2.66 which was determined as per ASTM standard procedure C136 [30]. Coarse aggregates (C.A) were obtained from the Margalla hills deposit which is considered one of the best sources in Pakistan. The aggregate size ranged from 9–12 mm. The properties of aggregates are given in Table 2.

3.1.3. Marble Powder

The marble powder (MP) was obtained from the local marble industry. The waste was produced by processing marble stone which includes cutting, shaping, and polishing collected in a settling basin. The MP was light grey in color and checked for clumps and impurities. The utilization of MP and strength of concrete depends upon the physical and chemical properties of MP. The chemical properties of MP are given in Table 1 and physical properties are listed in Table 2. The MP in this research was used as filler material [25].

3.1.4. Carbon Nano Tubes (CNTs)

The advance material used in this research was multiwalled carbon nanotubes (MWCNTs) which exhibit a high modulus of elasticity compared to steel. The physical and chemical properties of MWCNTs are provided in Table 3. In this study, the scattering of CNTs was carried out using polycarboxylate as a superplasticizer and sonicator, an electrically operated device [31]. The dispersion (sonication) time of MWCNTs in the sonicator was maintained constant at about 40 min. For the initial five minutes, a polycarboxylate-based superplasticizer at 0.008% by weight of cement was added in water in sonication bath which is responsible for optimum and uniform dispersion of CNTs. Then after every 8 min, an equal amount of CNTs was added to the sonication bath. After 40 min, the sonicated water was used for concrete casting. The MWCNTs are shown in Figure 1.

Table 3. Physio-chemical properties of MWCNTs.

Physical Property	Value/Specifications	Chemical Properties (Compounds)	Sample % Age by Wt.
Form	Powder form	Al_2O_3	7.01
Color	Black	SiO_2	0.53
Carbon Purity	Min. 95%	SO_3	0.46
Number of Walls	3–15	P_2O_5	0.44
Outer Diameter	5–20 nm	Fe_2O_3	0.18
Inner Diameter	2–6 nm	Loss on ignition	91.18
Apparent Density	0.15–0.35 g/cm^3	CaO	0.11
Flash Point	290 °C	CO_2O_3	0.09
Length	20–100 µm	Tm_2O_3	0.01
Water	Insoluble	K_2O	–
Density at 20 °C	0.15 g/cm^3	TiO_2	–
Danger of Explosion	At concentration 50 g/m^3 or higher	Specific surface area (m^2/kg)	250–300 (m^2/kg)

(**before**) (**after**)

Figure 1. Carbon nanotubes (CNTs) (**before**) and (**after**) being added to water.

3.2. Casting of Concrete Specimen

For compression testing, six types of reinforced concrete square columns having a size (150 mm × 150 mm × 600 mm) were cast adding MWCNTs and MP with the cement-aggregate ratio of 1:1.5:3. Two reference samples with no CNTs and MP were also developed for comparison purposes. It is worth mentioning that the average of three tested samples of each column type was taken for axial compression that complies with American Concrete Institute (ACI) 318-19 section 26.12.3.1 [32]. The w/c ratio was kept constant as 0.45 for all the concrete mixes to maintain sufficient workability. The columns were

equipped with four #3 (9.525 mm dia.) longitudinal bars and five #2 (6.4 mm dia.) bars as shear stirrups.

The elevation and cross-section are shown in Figure 2. The steel grade was labeled as grade 60 having a modulus of elasticity of 200 GPa and yield strength of 413.6 MPa. The length of the main bars for all columns was 571.5 mm, and that of shear stirrups was 533.4 mm.

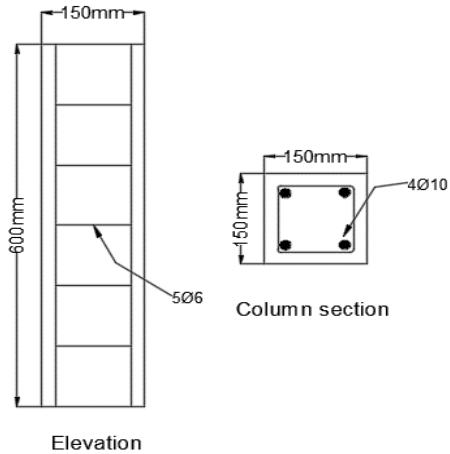

Figure 2. Column detailing.

The concrete columns were cast and cured in a water tank for 28 days. Similar mix proportioning was used in casting concrete cubes of standard size (150 mm × 150 mm × 150 mm). The cubes were cured for 7 days and 28 days in a water bath at room temperature. For all mixes, the ratio and size of the aggregate, cement content, and w/c ratio were kept constant. The concentration of MWCNTs varied between 0.025 to 0.2% in RC columns specimens, whereas the C1, C2, C3, C4, C5, and C6 mixes contain 0.025, 0.05, 0.075, 0.1, 0.15, 0.2% of MWCNTs with respect to cement weight. However, the amount of MP was kept constant as 5% by weight of cement for all mixes except control mix C0 with no MP content. The detail of mix proportions is presented in Table 4.

Table 4. Detail of mix proportions of RC columns.

Column ID	Cement (kg)	F.A (kg)	C.A(kg)	MP (kg)	CNTs (g)	w/c Ratio	Slump mm
C0	3.62	5.4	9	0	0	0.45	76
C0M5	3.62	5.4	9	0.18	0	0.45	79
C1	3.62	5.4	9	0.18	0.905	0.45	82
C2	3.62	5.4	9	0.18	1.81	0.45	88
C3	3.62	5.4	9	0.18	2.715	0.45	90
C4	3.62	5.4	9	0.18	3.62	0.45	95
C5	3.62	5.4	9	0.18	5.43	0.45	97
C6	3.62	5.4	9	0.18	7.24	0.45	99

3.3. Test Setup for Columns

The concrete columns were tested under axial compression in the compression testing machine. The machine was properly calibrated before use. The strain gauges, Linear Displacement Sensors (LDS) also called (LVDTs) were managed to attach at the front and back faces of the column. The P3 recorder (data logger) was used to store this data in 4 channels for accuracy purposes and then transmitted it to another external computer. The applied load data was stored by the Motor Control Centre (MCC) machine as shown in Figure 3. The whole assembly setup displayed the ultimate failure load of the short RC column and its corresponding strains (deflections) at every increment of 50 KN load.

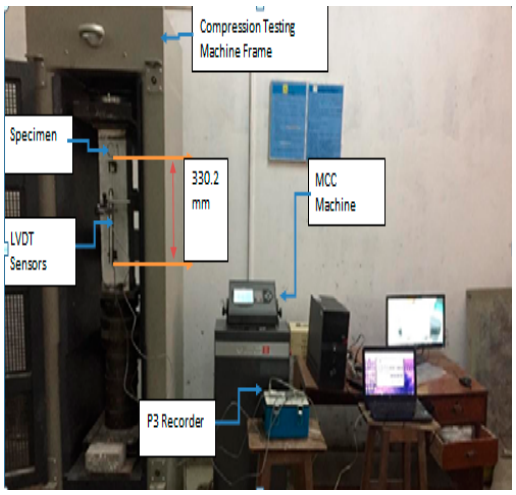

Figure 3. Test setup and record system.

4. Results and Discussion

4.1. SEM

The SEM analysis for the mixes is shown in Figure 4, which shows that a compact bridge structure is formed by adding CNTs in concrete mixes. Figure 4a showed visible folds between 90–100 layers which confirm a compact bridge structure responsible for the high strength of the C6 mix. These folds provide resistance to external loads which prevent cracking. Figure 4b shows the internal structure of the control mix in which no folds are formed and there is no bridge effect confirmed which leads to micro cracking as shown in the highlighted area.

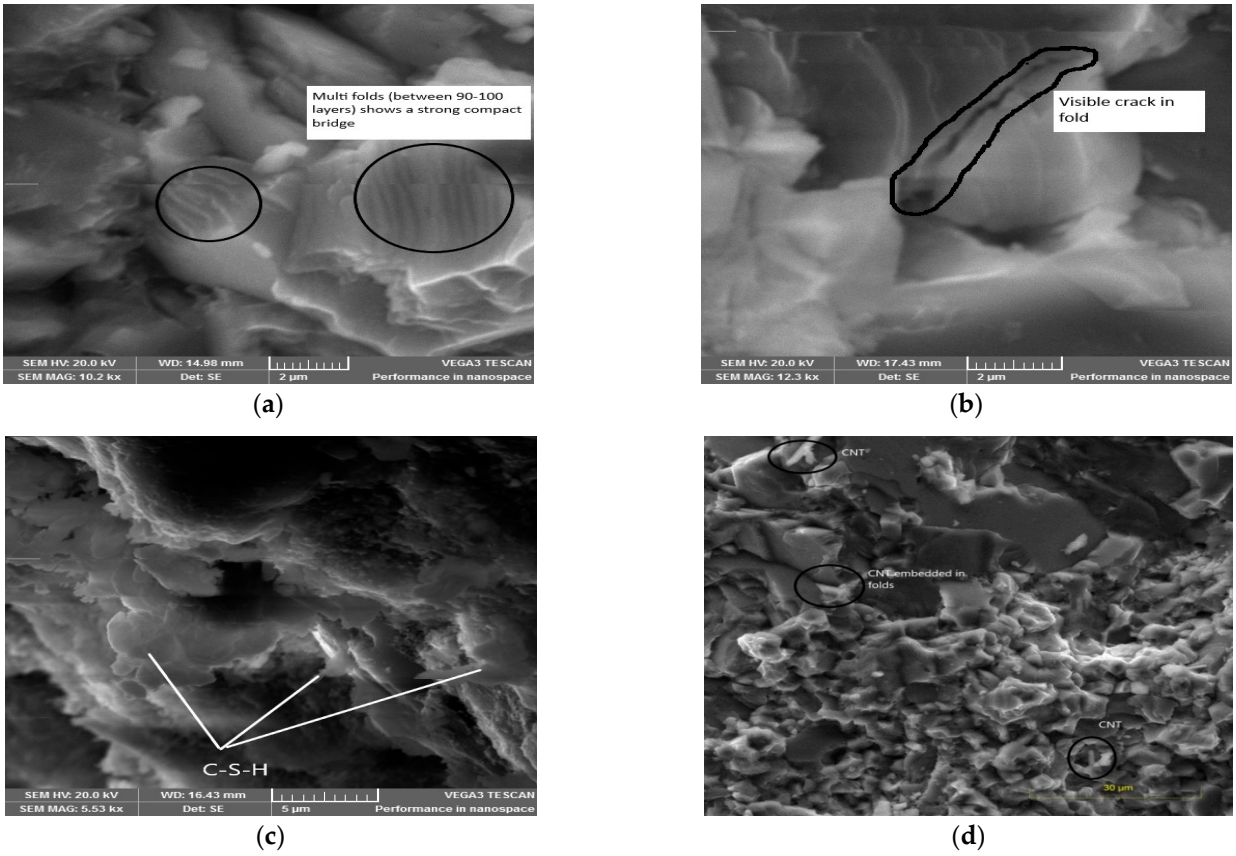

Figure 4. SEM analysis of C6 and C0 column (**a**) Folds in C6 mix (**b**) Crack appearance in the control mix (**c**) Formation of C-S-H gel in C6 Column (**d**) CNTs embedded in folds of C6 column.

Another reason for the high strength of CNT mixes is the formation of C-S-H gel which can be confirmed from Figure 4c. The highlighted portion shows that mixes with CNTs exhibit a high amount of C-S-H gel. The CNTs are tightly inserted between the hydrated products in the matrix because CNTs act as a nucleating agent for C-S-H gel as reported by [33]. SEM micrograph of C6 mix (Figure 4d) shows that CNTs were well dispersed by sonication method before mixing of concrete constituents. Also, the CNTs were found to develop a bridging effect within the cement paste microstructure to enhance the crack capturing ability, thus increasing the ultimate strength of the cement paste matrix. Hence, the ultra-strong MWCNTs appeared to cause significantly higher strength properties by the crack bridging effect.

4.2. Compressive Strength of Concrete Cubes

The results show that the compressive strength of concrete cubes increased with increasing content of MWCNTs which are shown in Figure 5. Also, compressive strength tends to increase with curing age. For instance, the mix C1 (having 0.025% of MWCNTs and 5% MP) has 7 days strength as 19.59 MPa while for 28 days the strength noted was 25.41 MPa, which shows a 29.70% increase in strength with curing age. The highest increase in strength was noted for mix C6 where the strength difference is 38.36% for 7 days and 28 days curing period. The increase in strength may be attributed to the optimum nucleating action of MWCNTs to facilitate the precipitation of hydration products by surrounding MWCNTs all around [34]. Moreover, MWCNTs interconnect the microstructure by bridging effect, preventing the generation of micro-cracking which is depicted in SEM analysis.

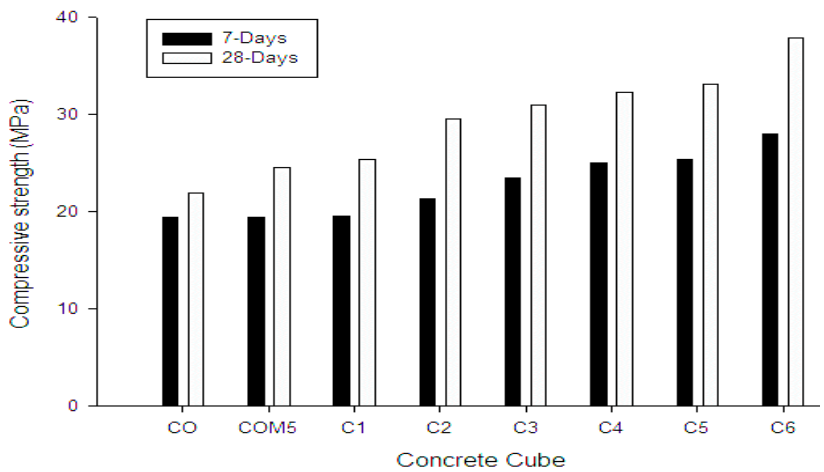

Figure 5. Variations of compressive strength of concrete cubes.

The mixes reinforced with MWCNTs show a significant increase in compressive strength compared to that of the control mix. The 7 days strength noted for mixes C1, C2, C3, C4, C5, and C6 were 19.59, 21.32, 23.47, 24.98, 25.41, and 28.00 MPa, respectively, whereas the strength at 28 days of curing was 25.41, 29.50, 31.00, 32.25, 33.16 MPa and 37.90 MPa respectively. It is shown that the highest compressive strength was noted for mix C6 for both 7 days and 28 days curing, which shows a higher trend than the control mix by 44.47% at 7 days and 72.58% at 28 days. The variations are given in Figure 5.

Literature [35] has also suggested the increase of compressive strength of cement paste composite with the inclusion of MWCNTs, the results indicated a 31% increase of compressive strength with the incorporation of 3% of MWCNTs. The MP has a positive effect on the properties of MWCNTs additive concrete. However, the strength increase was more pronounced at 28 days curing rather than 7 days curing. This is because of the synergic action of nucleation and filler effect in which MP provides nucleation sites for crystallization of C-S-H gel and fill the micro-sized pores in cement paste matrix, respectively [36]. The reactive nature of MP in the form of dolomite mineral lead to

the formation of calcium hydroxide and increases the alkalinity, which accelerated the hydration process by reducing the barrier of nucleation sites. It has been reported in the literature that the MP used in small quantities from 5 to 15% has more ability to fill the voids in concrete and improve the packing density of mixes [37]. Therefore, the compressive strength of concrete increased due to the bridging effect of MWCNTs, filler effect, and pronounced alkalinity due to the presence of MP.

4.3. Axial Behaviour of RC Columns

The compressive strength values of reinforced concrete columns at the curing age of 28 days are shown in Figure 6. The ultimate compressive strength of the control sample was recorded as 22.09 MPa at the point of fracture. The C0M5 concrete column (0% CNTs and 5% MP) showed ultimate compressive strength at 24.04 MPa which was recorded from the stress-strain curve. This showed that the compressive strength of the C0M5 column is greater than that of the control column by 8.11%. The reason may be explained as micro-sized particles of MP filled the voids in concrete and behaved as a compact cement paste matrix offering a higher load-carrying capacity of C0M5 column than reference specimen. The ultimate compressive strength of the RC columns specimens with 0.025, 0.05, 0.075, 0.10, 0.15, and 0.20% concentration of MWCNTs was resulted as 29.38, 30.71, 30.16, 32.84, 37.11, and 39.69 MPa, respectively. This shows an increase in compressive strength of 33.00, 39.02, 50.01, 51.11, 67.99, and 79.67% for RC column specimens containing 0.025, 0.05, 0.075, 0.10, 0.15, and 0.20% MWCNTs respectively as compared to that of the reference column, while the increase in compressive strength of the MWCNTs incorporated mixes comparative to that of C0M5 mix was recorded as 22.21, 27.74, 25.45, 36.60, 54.36, and 65.09%, respectively.

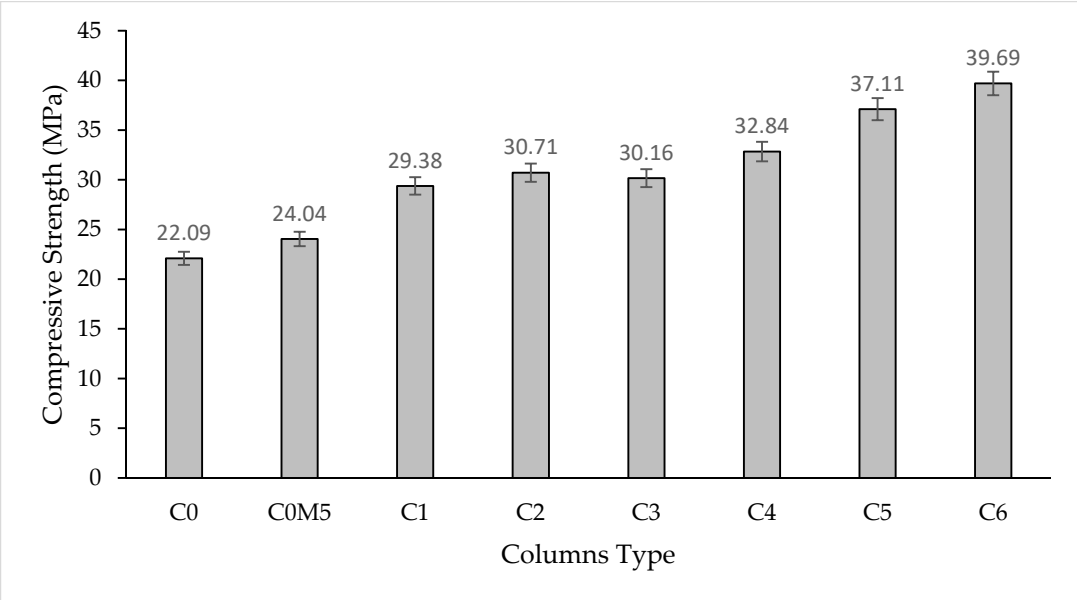

Figure 6. Ultimate axial compressive strength of different RC columns.

The exponential regression analysis between the percentage incorporation of MWCNTs and ultimate compressive strength of RC columns has been shown in Figure 7. The percentage addition of MWCNTs in the various mentioned mixes range between 0.023 to 0.188% weight of cement with the incremental size of 0.023%. The values of crushing strength of RC columns containing a concentration of MWCNTs that exist between the tested percentages can be interpolated using the following regression equation (Equation (1)) with considerable

accuracy as the value of the regression coefficient is around 0.91. The regression coefficient value indicates the good relation between data points and the regression curve.

$$\text{Compressive Strength of RC Columns} = 27.552\ e^{1.9401(\text{MWCNTs})} \quad (1)$$

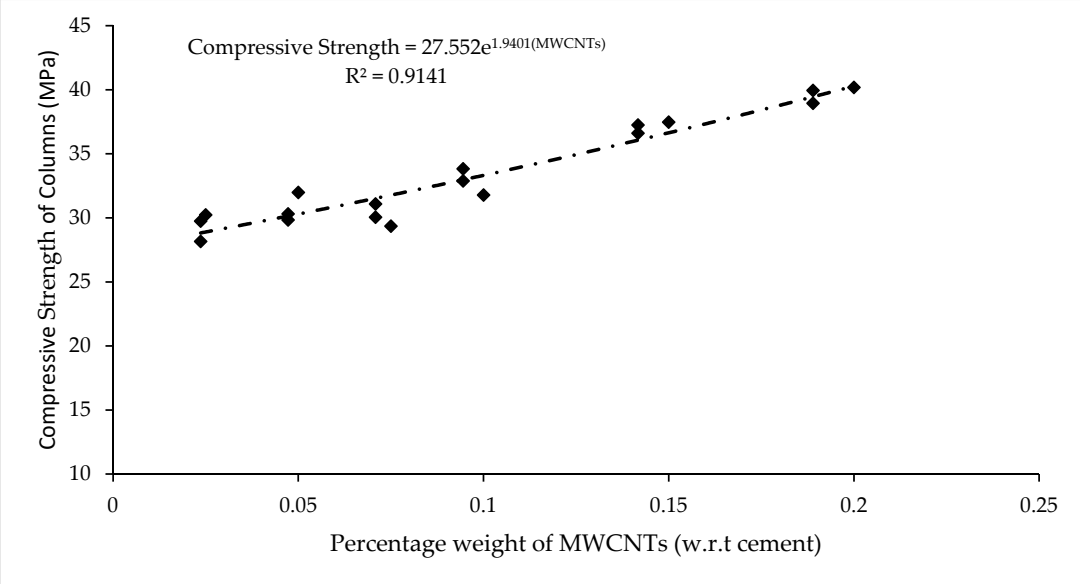

Figure 7. Strength development of RC columns upon incorporation MWCNTs.

The results show that adding MWCNTs enhances the compressive strength of RC columns together with MP. The increasing compressive strength values are also associated with the bridging effect of MWCNTs in concrete microstructure (SEM analysis), which may have withstood higher cracking (tensile) stresses compared to the control specimen. The highest strength value of 39.69 MPa was noted for sample C6 (0.20% MWCNTs and 5% MP), which was greater than the reference specimen by 79.67%. The incorporation of 0.2% of MWCNTs (C6 mix) in the RC column has shown an increase of 79.67% compressive strength as compared to that of the C0M5 column. The higher concentration of MWCNTs has provided more nucleation sites for the precipitation of hydration product, thus interlocking, and bridging within the microstructure to increase the load-carrying capacity of the C6 RC column in pure compression [38]. However, the surface energy of MWCNTs ranges between 27–45 mJ/m^2 which is responsible for bond existence between hydration product and MWCNTs [39]. The results of CNTs incorporating specimens strongly depend upon the dispersion of CNTs which provides a bridging effect between C-S-H gel and MWCNTs [40]. Another possible reason could be the small size of MWCNTs and MP which filled the pores of the concrete and behaved as compact mass and reduced capillary sorption. Therefore, the crack bridging effect due to the inclusion of MWCNTs and filler effect due to the presence of MP significantly improved the microstructure and enhance the load-carrying capacity.

4.4. Failure Modes

Failure of most of the RC columns with or without MWCNTs had similar behavior. The failure of the control column having no MWCNTs showed brittle behavior and sound cracking was observed during testing. In the early stage of load application, the column behaved similarly to columns with MWCNTs. In the elastic-plastic region, cracks appeared at the surface of the column which elongated to the top of the column and deep inside the column. Local buckling of longitudinal reinforcement was also observed. As the load progressed, the concrete cover was broken, and cracks propagated inside the column resulting in the concrete crushing and buckling of longitudinal reinforcement as shown in Figure 8.

(**a**) (**b**) (**c**)

Figure 8. Failure modes of control column (**a**) Buckling of longitudinal reinforcement (**b**) Crushing of column (**c**) Cracks Propagates deep inside.

The maximum load-carrying capacity was observed for column C6. In the early ages of load application, the C6 mix showed significant resistance against load, and no cracks have appeared at the surface of the concrete. The deformation of the column was very small compared to other columns in the elastic region. The first crack was appeared on the left top surface of the column and propagated to the bottom up to 70% of column length.

However, no buckling of reinforcement or opening of stirrups was observed at any stage of loading. When axial loads reached their peak values, delamination of concrete was observed on the surface where cracks appeared, and longitudinal reinforcement was exposed to the atmosphere. By closely observing column C6, it was noted that there were no cracks propagated beyond shear reinforcement as shown in Figure 9, which is indicative of the fact that the shear capacity of concrete increased significantly at 0.2% incorporation of MWCNTs in the RC column even at fracture. Moreover, the concrete confined within reinforcement did not undergo high deformations in the C6 column.

(**a**) (**b**)

Figure 9. Failure pattern of C6 column (**a**) Top surface of column is removed (**b**) No buckling or delamination of stirrups.

The RC column having no MWCNTs and 5% MP (C0M5) showed ductile failure. The difference between column C0M5 and C6 is that the former was crushed from both sides and later from the left side only. The exposure of longitudinal reinforcement and shear reinforcement was more visible in the C0M5 mix. The concrete bounded within reinforcement was crushed leading to buckling of longitudinal reinforcement. The delamination of concrete was severe from both sides as axial loads reached close to their peak values as shown in Figure 10.

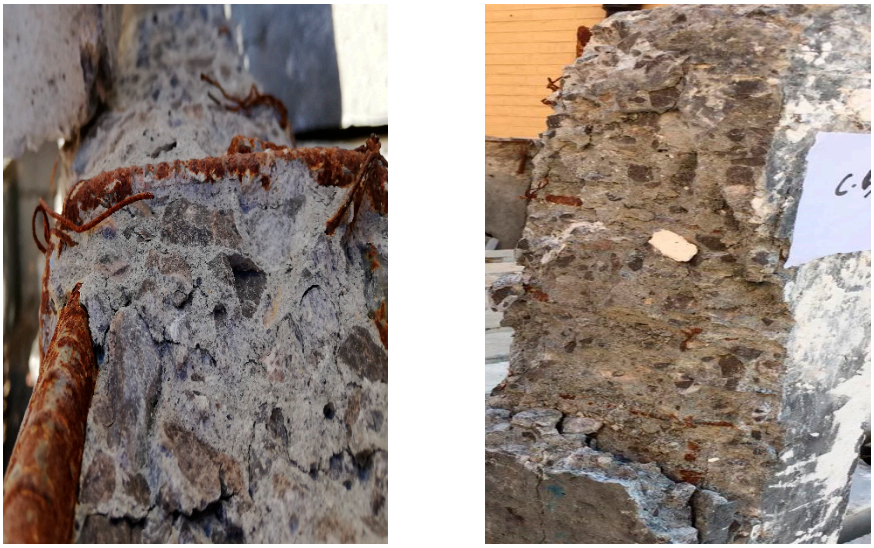

(**a**) (**b**)

Figure 10. Failure pattern of C0M5 column (**a**) Exposure of reinforcement (**b**) Spalling of concrete cover.

The RC columns containing 0.025, 0.05, 0.075, 0.10, 0.15, and 0.20% of MWCNTs had shown the crushing behavior with no buckling, whereas the control concrete under similar loading conditions had shown the crushing behavior. The cracking pattern and axial deformation are shown in Figure 11. The other parameters associated with columns during testing such as ultimate load, load-displacement, stiffness, and toughness are given in Table 5. The corresponding ultimate displacement, axial toughness of control (C0) and mix with the inclusion of MP (C0M5) was observed as 1.395 mm, 693.32 KN.mm and 1.311 mm, 412.66 KN.mm, respectively which depicts the drop in ductility of RC column specimen with the incorporation of MP despite the increased load-carrying capacity in C0M5 mix. The loss in ductility has resulted because MP act as filler in the concrete matrix, only enhancing its compressive strength, which has also been explained in SEM analysis. However, the ultimate displacement and axial toughness of RC columns increased upon the addition of MWCNTs which was due to its ultra-high tensile strength, crack capturing, and crack bridging properties.

4.5. Load-Deformation Behaviour

The load-deformation curves for all the beams with and without MWCNTs are shown in Figure 12. It may be noted that the stiffness of all the beams exhibited a similar trend at the initial stage of loading. For the control specimen, an ultimate load of 497 KN was noted for a deflection value of 1.395 mm. Beyond this stage, the stiffness tends to decrease. The decrease in stiffness was observed for all the columns having MWCNTs which increase linearly with increased content of MWCNTs.

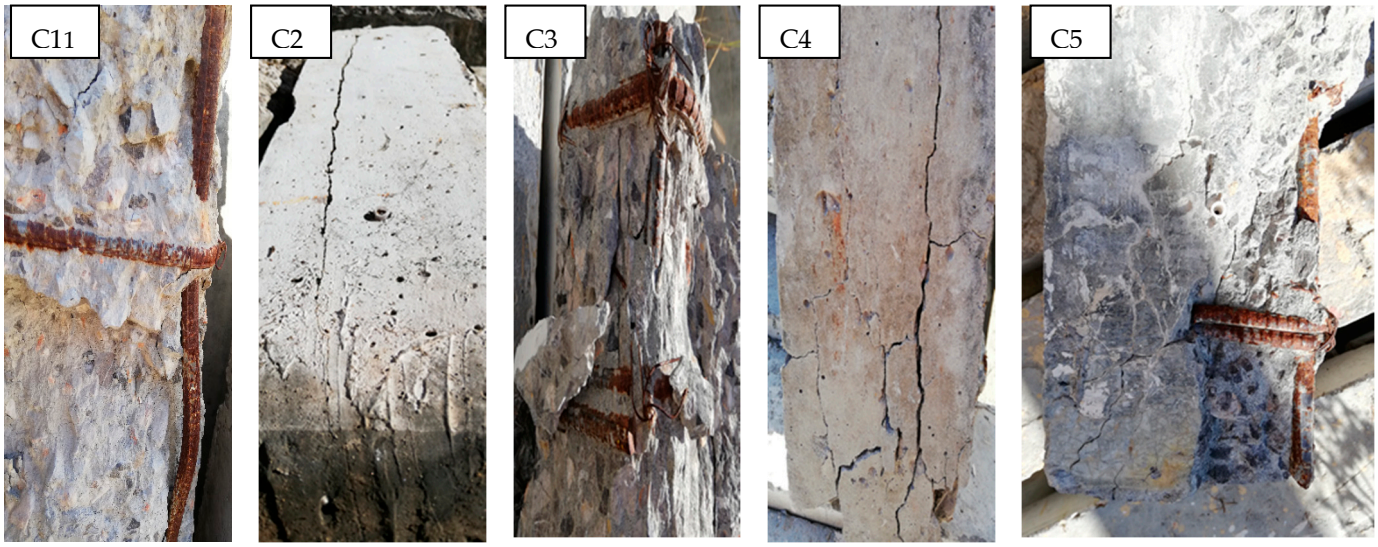

Figure 11. Failure modes of other columns.

Table 5. Parameters associated with the load-deflection curve.

Specimen	Ultimate Load (KN)	Ultimate Displacement (mm)	Initial Stiffness (KN/mm)	Toughness (KN.mm)	Failure Mode
C0	497	1.395	356.27	693.32	Buckling
C0M5	541	1.311	412.66	709.25	Crushing
C1	661	1.661	397.95	1097.92	Crushing
C2	691	1.713	403.39	1183.68	Crushing
C3	746	1.811	411.93	1351.01	Crushing
C4	739	1.781	414.94	1316.16	Crushing
C5	835	1.88	444.15	1569.80	Crushing
C6	893	1.99	448.74	1777.07	Crushing

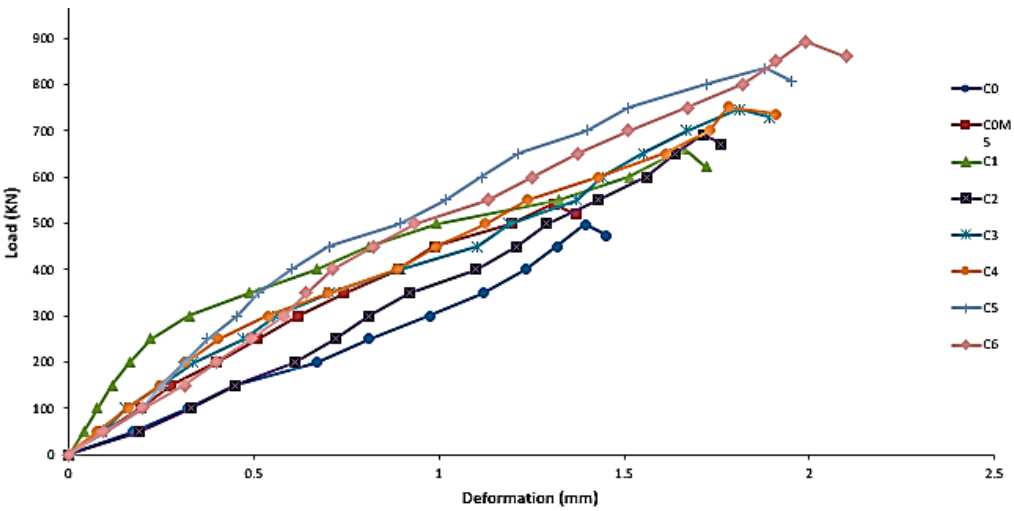

Figure 12. Comparison of load-deflection curves for all the columns.

The highest increase was noted for C6 (0.20% MWCNTs and 5% MP) column. The maximum deflection was noted as 1.99 mm at a loading of 892 KN. The increase may be attributed to the increasing content of MWCNTs which provided strong compact bridge and prevented concrete from cracking and spalling. The elongated shapes of MWCNTs together with MP as filler material provided resistance and became more efficient in the cracking zone. The maximum load was greater than the control specimen C0 by 79.6% and

more than the C0M5 mix by 65.06%. Therefore, the results indicated that the inclusion of MWCNTs strengthens the concrete microstructure, thus increase the load-carrying capacity significantly.

4.6. Ductility

The ductility of a structural member is the tendency to deform to a large strain without fracturing under the applied load. It provides a warning before the failure of a structural member. The ductility is the ratio of axial displacement to the 85% of ultimate load given in Equation (2) [41].

$$\mu = \varepsilon 0.85/0.004 \quad (2)$$

Where μ represents ductility and ε represents strain.

A column having greater areas under the stress-strain curve is considered a more ductile column. The ductility for the reference mix (C0) was found to be 1.056. It was found that ductility tends to increase by increasing MWCNTs. It was observed that the C0M5 column had the lowest ductility which means that MP had an adverse effect on ductility. The values of ductility observed for mixes C1, C2, C3, C4, C5, and C6 were greater than that of the reference mix by 18.37, 23.10, 30.20, 27.84, 34.94, and 42.04% respectively. The overall trend of ductility ratio is shown in Figure 13. The ductility value was found to be highest for mix C6. However, the lowest ductility was found for the mix C0M5 which is less than that of the reference column by 5.8%, the drop in ductility value was observed for C0M5 specimens due to the reason that MP had not contributed chemically to the cement paste matrix, however, MP behaved as a filler in cement paste matrix only enhancing compressive strength with the expense of losing ductility and attributing brittleness to the concrete.

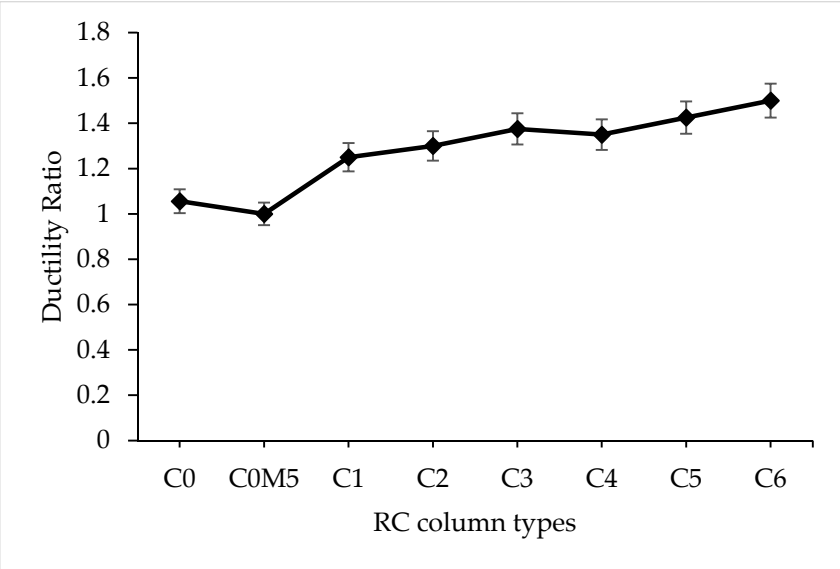

Figure 13. Variations of ductility with RC column type.

The stress-strain curves for all RC columns are given in Figure 14. The previous studies show that the addition of MWCNTs increased the ductility values of concrete at the age of 28 days and resulted in high energy absorption. The ductility value strongly depends upon the concentration, curing time, and dispersion of MWCNTs in the mix [42]. A significant increase in ductility ratio was noted in MWCNTs reinforced concrete which shows an increase in the area under the stress-strain curve allowing more energy dissipation in this region [35]. It is known in several literature studies that the inclusion of short fiber in brittle material such as concrete impart ductile behavior [43], therefore the incorporation of MWCNTs in cement composite increased the ductility of the RC column.

Therefore, the ductility of the RC column increased due to the ultra-high tensile strength of incorporated MWCNTs.

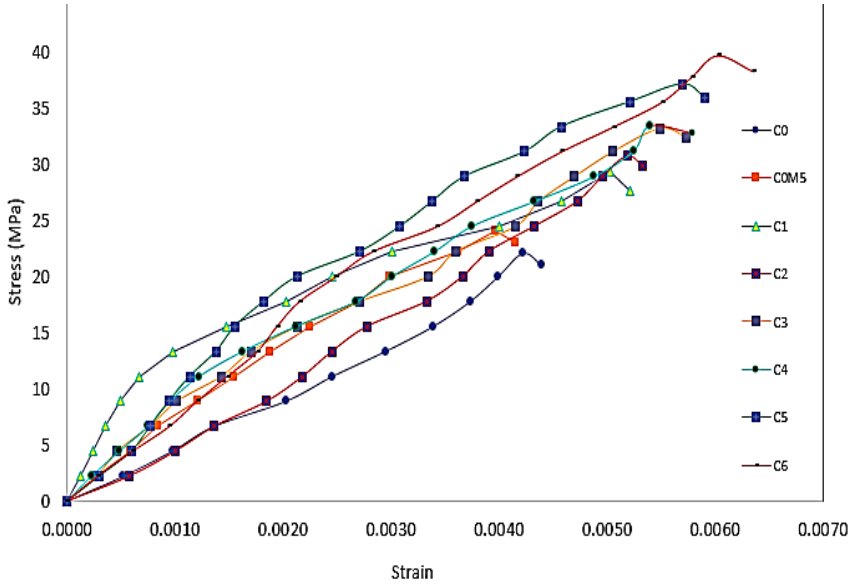

Figure 14. Comparison of stress-strain curves of all RC columns.

5. Conclusion and Recommendations

5.1. Conclusions

In this study, an attempt was made to use multi-walled carbon nanotubes in reinforced concrete columns to assess mainly its axial properties of the reinforced column. The following conclusions can be drawn from the above study:

1. The MWCNTs incorporating columns tend to increase the axial compressive strength. The highest strength was noted for the column (0.20% MWCNTs & 5% marble powder) which was found more than the reference column by 79.11%.
2. By adding CNTs in the concrete increases its strength with curing age as noted in the case of concrete cubes. It was noted that concrete cubes incorporated with 0.20% CNTs and 5% marble powder had greater strength than reference mix by 44.47, 72.58% at 7, and 28 days of curing, respectively.
3. The incorporation of MWCNTs in concrete enhanced its microstructure and strength to minimize column buckling. There was no buckling of reinforcement observed in columns cast with adding MWCNTs except for columns having 0.025% CNTs & 5% marble powder.
4. The load-deflection curves confirm maximum stiffness for MWCNTs columns and minimum for control columns.
5. The columns incorporated with 0.20% MWCNTs exhibit higher ductility than the control specimen by 42.04%.
6. The columns incorporated with no MWCNTs and 5% marble powder showed ductile failure.
7. The SEM analysis confirms the bridging formation of MWCNTs in the form of folds and layers embedded in the concrete matrix.
8. The SEM analysis also confirms the embedding of MWCNTs in the C-S-H gel.

5.2. Recommendations

The incorporation of 0.20% MWCNTs and 5% marble powder as filler material by weight of cement are recommended to be effectively used as a reinforcing agent in concrete.

At structural level, the strain sensing attribute of MWCNTs can be utilized to study the actual performance of column in seismic event and it may open up the venues in structural

health monitoring. However, at microstructural level, Nuclear Magnetic Resonance (NMR) spectroscopy may be used to develop the quantitative understanding for development of hydration phases of MWCNTs cement composite containing Marble Powder.

Author Contributions: Conceptualization, A.J.K. and L.A.Q.; Data curation, A.J.K., A.G., M.U. and A.A.; Formal analysis, A.J.K., M.N.A.K., A.G., M.U. and U.J.; Methodology, A.J.K., A.M., Y.I.B. and A.A.; Investigation, A.J.K., M.N.A.K., A.M. and Y.I.B.; Software, A.J.K.; Writing—Original draft, A.J.K. and M.N.A.K.; Supervision, L.A.Q. and R.F.; Visualization, U.J. and R.F.; Writing—Review & Editing, U.J. and R.F. All authors have read and agreed to the published version of the manuscript.

Funding: This research received no external funding.

Institutional Review Board Statement: Not applicable.

Informed Consent Statement: Not applicable.

Data Availability Statement: The data presented in this study are available on request from the corresponding authors.

Acknowledgments: The authors are thankful to concrete Laboratory officials of Civil Engineering Department University of Engineering & Technology Taxila, Pakistan for helping in conducting experiments.

Conflicts of Interest: The authors declare no conflict of interest.

Abbreviations

C0 (0% CNTs & 0% MP), COM5 (0% CNTs & 5% MP), C1 (0.025% CNTs & 5% MP), C2 (0.050% CNTs & 5% MP), C3 (0.075 % CNTs & 5% MP), C4 (0.10 % CNTs & 5% MP), C5 (0.150% CNTs & 5% MP), C6 (0.20% CNTs & 5% MP), SEM (Scanning Electron Microscopy); C-S-H (Calcium Silicate Hydrate).

References

1. Yakovlev, G.; Pervushin, G.; Maeva, I.; Keriene, J.; Pudov, I.; Shaybadullina, A.; Buryanov, A.; Korzhenko, A.; Senkov, S. Modification of Construction Materials with Multi-Walled Carbon Nanotubes. *Procedia Eng.* **2013**, *57*, 407–413. [CrossRef]
2. Tamimi, A.; Hassan, N.M.; Fattah, K.; Talachi, A. Performance of cementitious materials produced by incorporating surface treated multiwall carbon nanotubes and silica fume. *Constr. Build. Mater.* **2016**, *114*, 934–945. [CrossRef]
3. Eftekhari, M.; Mohammadi, S.; Khanmohammadi, M. A hierarchical nano to macro multiscale analysis of monotonic behavior of concrete columns made of CNT-reinforced cement composite. *Constr. Build. Mater.* **2018**, *175*, 134–143. [CrossRef]
4. Douba, A.; Emiroglu, M.; Kandil, U.F.; Taha, M.M.R. Very ductile polymer concrete using carbon nanotubes. *Constr. Build. Mater.* **2019**, *196*, 468–477. [CrossRef]
5. Reis, J.M.L.D. Mechanical Characterization of Fiber Reinforced Polymer Concrete. *Mater. Res.* **2005**, *8*, 357–360. [CrossRef]
6. Saeed, H.Z.; Khan, H.A.; Farooq, R. Experimental investigation of stress–strain behavior of CFRP confined Low Strength Concrete (LSC) cylinders. *Constr. Build. Mater.* **2016**, *104*, 208–215. [CrossRef]
7. Lee, H.; Kang, D.; Kim, J.; Choi, K.; Chung, W. Void detection of cementitious grout composite using single-walled and multi-walled carbon nanotubes. *Cement Concr. Compos.* **2019**, *95*, 237–246. [CrossRef]
8. Iijima, S.; Ichihashi, T. Single shell Carbon nanotubes of 1-nm diameter. *Nature* **1993**, *363*, 603–605. [CrossRef]
9. Gillani, S.S.U.H.; Khitab, A.; Ahmad, S.; Khushnood, R.A.; Ferro, G.A.; Kazmi, S.M.S.; Qureshi, L.A.; Restuccia, L. Improving the mechanical performance of cement composites by carbon nanotubes addition. *Procedia Struct. Integr.* **2017**, *3*, 11–17. [CrossRef]
10. Hadavand, B.S.; Javid, K.M.; Gharagozlou, M. Mechanical properties of multi-walled carbon nanotube / epoxy polysulfide nanocomposite. *Mater. Des.* **2013**, *50*, 62–67. [CrossRef]
11. Geng, Y.; Liu, M.Y.; Li, J.; Shi, X.M.; Kim, J.K. A Effects of surfactant treatment on mechanical and electrical properties of CNT / epoxy nanocomposites. *Compos. Part A Appl. Sci. Manuf.* **2008**, *39*, 1876–1883. [CrossRef]
12. Shokrieh, M.M.; Rafiee, R. Investigation of nanotube length effect on the reinforcement efficiency in carbon nanotube-based composites. *Compos. Struct.* **2010**, *92*, 2415–2420. [CrossRef]
13. Yu, M.F.; Lourie, O.; Dyer, M.J.; Moloni, K.; Kelly, T.F.; Ruoff, R.S. Strength and Breaking Mechanism of Multiwalled Carbon Nanotubes Under Tensile Load. *Science* **2000**, *287*, 637–640. [CrossRef]
14. Li, G.Y.; Wang, P.M.; Zhao, X. Mechanical behavior and microstructure of cement composites incorporating surface-treated multi-walled carbon nanotubes. *Carbon* **2005**, *43*, 1239–1245. [CrossRef]
15. Cwirzen, A.; Habermehl-Cwirzen, K.; Penttala, V. Surface decoration of carbon nanotubes and mechanical properties of cement/carbon nanotube composites. *Adv. Cem. Res.* **2008**, *20*, 65–73. [CrossRef]

16. Torkittikul, P.; Chaipanich, A. Bioactivity and Mechanical Properties of White Portland Cement Paste with Carbon Nanotubes. In Proceedings of the 3rd International Nanoelectronics Conference (INEC), Hong Kong, China, 3–8 January 2010. [CrossRef]
17. Chaipanich, A.; Nochaiya, T.; Wongkeo, W.; Torkittikul, P. Compressive strength and microstructure of carbon nanotubes—fly ash cement composite. *Mater. Sci. Eng. A* **2010**, *527*, 1063–1067. [CrossRef]
18. Konsta-Gdoutos, M.S.; Metaxa, Z.S.; Shah, S.P. Cement and Concrete Research Highly dispersed carbon nanotube reinforced cement-based materials. *Cem. Concr. Res.* **2010**, *40*, 1052–1059. [CrossRef]
19. Xie, X.L.; Mai, Y.W.; Zhou, X.P. Dispersion, and alignment of carbon nanotubes in polymer matrix: A review. *Mater. Sci. Eng. R Rep.* **2006**, *49*, 89–112. [CrossRef]
20. Suchorzewski, J.; Prieto, M.; Mueller, U. An experimental study of self-sensing concrete enhanced with multi-wall carbon nanotubes in wedge splitting test and DIC. *Constr. Build. Mater.* **2020**, *262*, 120871. [CrossRef]
21. Akbar, A.; Liew, K.M.; Farooq, F.; Khushnood, R.A. Exploring mechanical performance of hybrid MWCNT and GNMP reinforced cementitious composites. *Constr. Build. Mate.* **2021**, *267*, 120721. [CrossRef]
22. Singh, N.B.; Kalra, M.; Saxena, S.K. Nanoscience of cement and concrete. *Mater. Today. Proc.* **2017**, *4*, 5478–5487. [CrossRef]
23. Baloch, W.L.; Khushnood, R.A.; Khaliq, W. Influence of multi-walled carbon nanotubes on the residual performance of concrete exposed to high temperatures. *Constr. Build. Mater.* **2018**, *185*, 44–56. [CrossRef]
24. Munir, M.J.; Kazmi, S.M.S.; Wu., Y.-F. Efficiency of waste marble powder in controlling alkali–silica reaction of concrete: a sustainable approach. *Constr. Build. Mater.* **2017**, *154*, 590–599. [CrossRef]
25. Tunc, E.T. Recycling of marble waste: A review based on strength of concrete containing marble waste. *J. Environ. Manag.* **2019**, *231*, 86–97. [CrossRef] [PubMed]
26. Corinaldesi, V.; Moriconi, G.; Naik, T.R. Characterization of marble powder for its use in mortar and concrete. *Constr. Build. Mater.* **2010**, *24*, 113–117. [CrossRef]
27. Hebhoub, H.; Aoun, H.; Belachia, M.; Houari, H.; Ghorbel, E. Use of waste marble aggregates in concrete. *Constr. Build. Mater.* **2011**, *25*, 1167–1171. [CrossRef]
28. Silva, D.; Gameiro, F.; de Brito, J. Mechanical Properties of Structural Concrete Containing Fine Aggregates from Waste Generated by the Marble Quarrying Industry. *J. Mater. Civ. Eng.* **2014**, *26*, 1–8. [CrossRef]
29. *ASTM C150/C150M-19a, Standard Specification for Portland Cement*; ASTM International: West Conshohocken, PA, USA, 2019; Available online: www.astm.org (accessed on 9 February 2021).
30. *ASTM C136/C136M-14, Standard Test Method for Sieve Analysis of Fine and Coarse Aggregates*; ASTM International: West Conshohocken, PA, USA, 2014; Available online: www.astm.org (accessed on 9 February 2021).
31. Ma, P.C.; Siddiqui, N.A.; Marom, G.; Kim, J.K. Dispersion, and functionalization of carbon nanotubes for polymer-based nanocomposites: A review. *Compos. Part A Appl. Sci. Manuf.* **2010**, *41*, 1345–1367. [CrossRef]
32. *ACI 318-19, Building Code Requirements for Structural Concrete and Commentary*; American Concrete Institute (ACI): Farmington Hills, MI, USA, 2019.
33. Parveen, S.; Rana, S.; Fangueiro, R.; Paiva, M.C. Microstructure and mechanical properties of carbon nanotube reinforced cementitious composites developed using a novel dispersion technique. *Cem. Concr. Res.* **2015**, *73*, 215–227. [CrossRef]
34. Sedaghatdoost, A.; Behfarnia, K.; Bayati, M. The effect of curing period on the residual strength of Portland cement mortar containing MWCNTs at elevated temperature. *Constr. Build. Mater.* **2019**, *196*, 144–153. [CrossRef]
35. Eftekhari, M.; Mohammadi, S. Multiscale dynamic fracture behavior of the carbon nanotube reinforced concrete under impact loading. *Int. J. Impact Eng.* **2016**, *187*, 55–64. [CrossRef]
36. Li, L.G.; Huang, Z.H.; Tan, Y.P.; Kwan, A.K.H.; Chen, H.Y. Recycling of marble dust as paste replacement for improving strength, microstructure and eco-friendliness of mortar. *J. Cleaner Prod.* **2018**, *210*, 55–65. [CrossRef]
37. Kabeer, K.S.A.; Vyas, A.K. Utilization of marble powder as fine aggregate in mortar mixes. *Constr. Build. Mater.* **2018**, *165*, 321–332. [CrossRef]
38. Thomas, J.J.; Jennings, H.M.; Chen, J.J. Influence of Nucleation Seeding on the Hydration Mechanisms of Tricalcium Silicate and Cement. *J. Phys. Chem. C* **2009**, *113*, 4327–4334. [CrossRef]
39. Miled, K.; Sab, K.; Le Roy, R. Particle size effect on EPS lightweight concrete compressive strength: Experimental investigation and modelling. *Mech. Mater.* **2007**, *39*, 222–240. [CrossRef]
40. Carriço, A.; Bogas, J.A.; Hawreen, A.; Guedes, M. Durability of multi-walled carbon nanotube reinforced concrete. *Constr. Build. Mater.* **2018**, *164*, 121–133. [CrossRef]
41. Shanan, M.A.; El-zanaty, A.H.; Metwally, K.G. Effect of Concrete Strength and Aspect Ratio on Strength and Ductility of Concrete Columns. *IJCEE* **2016**, *10*, 955–963. [CrossRef]
42. Rashad, A.M. Effect of carbon nanotubes (CNTs) on the properties of traditional cementitious material. *Constr. Build. Mater.* **2017**, *153*, 81–101. [CrossRef]
43. Jang, A.Y.; Lim, S.H.; Kim, D.H.; Yun, H.D.; Lee, G.C.; Seo, S.Y. Strain-Detecting properties of hybrid PE and steel fibers reinforced cement composite (Hy-FRCC) with Multi-Walled carbon nanotube (MWCNT) under repeated compression. *Results Phys.* **2020**, *18*, 103199. [CrossRef]